

Constraints from v_2 fluctuations for the initial state geometry of heavy-ion collisions

Thorsten Renk and Harri Niemi

*Department of Physics, P.O. Box 35, FI-40014 University of Jyväskylä, Finland and
Helsinki Institute of Physics, P.O. Box 64, FI-00014 University of Helsinki, Finland*

The ability to accurately compute the series of coefficients v_n characterizing the momentum space anisotropies of particle production in ultrarelativistic heavy ion collisions as a function of centrality is widely regarded as a triumph of fluid dynamics as description of the bulk matter evolution. A key ingredient to fluid dynamical modeling is however the initial spatial distribution of matter as created by a yet not completely understood equilibration process. A measurement directly sensitive to this initial state geometry is therefore of high value for constraining models of pre-equilibrium dynamics. Recently, it has been shown that such a measurement is indeed possible in terms of the event by event probability distribution of the normalized v_n distribution as a function of centrality, which is to high accuracy independent on the details of the subsequent fluid dynamical evolution and hence directly reflects the primary distribution of spatial eccentricities. We present a study of this observable using a variety of Glauber-based models and argue that the experimental data place very tight constraints on the initial distribution of matter and rule out all simple Glauber-based models.

PACS numbers: 25.75.-q, 25.75.Gz

I. INTRODUCTION

It is now commonly agreed that ultrarelativistic heavy-ion (A-A) collisions create a transient state of collective QCD matter. In modeling the dynamics of this droplet, the essential input to the models is an initial distribution of matter density as created in a yet not completely understood equilibration process [1]. One of the clearest signal of collective (or fluid dynamical) behavior of such a system is the appearance of non-trivial patterns in the azimuthal distribution of final state hadron spectra [2]. Such patterns are created by the fluid dynamical response to pressure gradients which in turn are given by the geometric shape of the initial state [3, 4]. The precise details of this response then depend strongly on the transport properties of the matter, e.g. shear viscosity [5–15].

The azimuthal asymmetries of the measured hadron momentum spectra are usually characterized by the set of Fourier coefficients v_n , and similarly the azimuthal distribution of matter in position space can be characterized by its eccentricity coefficients ε_n . The determination of the viscosity of the strongly interacting matter is largely based on measured v_n 's. However, v_n 's do not only depend on the fluid dynamical response to ε_n 's, but also on the initial values of ε_n 's. Therefore, it is essential that the right initial condition is used: determining both the transport properties and the initial geometry simultaneously from the available data is a very complicated task [16, 17]. Thus, finding an observable that is sensitive to the initial geometry, but independent of the fluid dynamical response would simplify the task considerably. Another phenomena where the detailed knowledge of the initial geometry becomes important is jet quenching, where the observed azimuthal jet suppression patterns depend strongly on the assumed initial state [18, 19].

In realistic modeling, the initial state geometry fluctuates from one collision to the another even for a fixed im-

pact parameter [20, 21]. The event-by-event fluctuations of ε_n 's then translate into the event-by-event fluctuations of v_n 's. Fluid dynamical calculations have established that the relation $\langle v_n \rangle = C_n \varepsilon_n$, where the angular brackets $\langle \rangle$ denote the average over many collisions with the same eccentricity, holds very well [22–25]. For the second harmonics v_2 and ε_2 it has been found that the correlation is even stronger and a relation $v_2 = C_2 \varepsilon_2$ holds accurately also in individual nuclear collisions [25], not only on average. This means that in a given centrality class ε_2 is the only characteristics of the initial condition that determines v_2 , while the proportionality coefficient C_2 depends on the details of the fluid dynamical evolution in a complicated way [26]. The simple relation means that in relative fluctuations $\delta v_2 = (v_2 - \langle v_2 \rangle) / \langle v_2 \rangle$ the proportionality coefficient cancels. Therefore, the probability distribution $P(\delta \varepsilon_n)$ is the same as the probability distribution $P(\delta v_n)$. In other words $P(\delta v_n)$ is determined by the properties of initial state alone and is independent of the fluid dynamical evolution. Thus, by measuring $P(\delta v_n)$ one gets an immediate access to the fluctuations in the initial geometry [25].

Recently, the event-by-event distributions of v_n have been measured by the ATLAS [27] and ALICE [28] Collaborations. Making use of the result $P(\delta \varepsilon_n) = P(\delta v_n)$ we use different variants of the Monte-Carlo Glauber (MCG) model to calculate $P(\delta \varepsilon_n)$, and compare with ATLAS data. Furthermore, we study the sensitivity of the distributions to several assumptions underlying the MCG model and its extensions.

II. THE MODEL

We compute the normalized fluctuations of v_n by evaluating the spatial eccentricity ε_n of a set of randomly generated initial states for a given centrality class.

We start by distributing the potentially interacting objects in the initial states of the colliding nuclei. In the default scenario, these are the nucleons, but in an alternative constituent quark scattering (CQS) scenario, we assume that the substructure of nucleons in terms of constituent quarks is the relevant level of description.

In the default case, we use a Woods-Saxon parametrization of the measured nuclear charge density [29] to distribute nucleons randomly in a 3-dim volume. For Pb-nuclei as appropriate for the LHC, our distribution is given by

$$\rho_N(r) = \frac{\rho_0}{1 + \exp((r - c)/z)} \quad (1)$$

with $c = 6.61$ fm and the skin thickness $z = 0.51$ fm. We checked that a slight changes in these parameters do not affect our result significantly. We do not correct for the nucleon hard core, i.e. we permit configurations in which individual nucleons overlap in 3d space. After generating a 3d ensemble of nucleons, we project their position into transverse (x, y) space. In the CQS scenario, we distribute three constituent quarks inside a Gaussian radius of 0.6 fm around the nominal position of each nucleon, then project constituent quark positions into (x, y) space.

In order to test alternative scalings, we also explore a Hard Sphere scenario (HS) in which we set the skin thickness parameter $z = 0$ and a Sheet (S) scenario in which we mimick a strongly saturated picture in which we distribute nucleons a priori into a 2d circular surface bounded by the nuclear radius parameter c (in such a picture, the center of the nucleus is as dense as the periphery). Both HS and S can be combined with the CQS scenario.

Once the transverse position of the colliding objects have been specified for two nuclei, we displace the two distributions by a randomly sampled impact parameter. Collisions are evaluated according to a transverse distance criterion $d^2 < \sigma_{NN}/\pi$. In the case of nucleon-nucleon collisions we take $\sigma_{NN} = 64$ mb, in the case of interacting constituent quarks we use 1/9 of this value to get back to the same cross section in the case of p-p collisions.

There are four common ways in which EbyE hydrodynamics is commonly initialized. Matter can be distributed either according to collision participants (wounded nucleon, WN) or according to binary collisions (BC) and the matter distribution can be specified in terms of entropy s or energy density e , leading to sWN, eWN, sBC and eBC scenarios. We note that none of these alone is able to give a correct centrality dependence of the multiplicity.

For each event, we associate a binary collision and a wounded nucleon density according to

$$\rho(\mathbf{x})_{\text{bin}/\text{wn}} = \sum_{i=1}^{N_{\text{bin}/\text{wn}}} \frac{1}{2\pi\sigma^2} \exp\left(-\frac{\mathbf{x}_i^2}{2\sigma^2}\right) \quad (2)$$

where \mathbf{x}_i is the binary collision point or the position of the wounded nucleon, and σ is a free parameter. We will

then consider three different possibilities to initialize the initial entropy density,

$$s(\mathbf{x}) = N\rho_{\text{bc}}(\mathbf{x})^\alpha, \quad (3)$$

$$s(\mathbf{x}) = N\rho_{\text{wn}}(\mathbf{x})^\beta, \quad (4)$$

$$s(\mathbf{x}) = N[(f\rho_{\text{wn}}(\mathbf{x}) + (1-f)\rho_{\text{bc}}(\mathbf{x})], \quad (5)$$

where the parameters α , β and f are fixed to reproduce the centrality dependence of the multiplicity, by assuming that the final multiplicity is proportional to the initial entropy. We have tested that scaling $s \rightarrow s^{4/3}$, corresponding to the approximate difference between s and e scaling, does not change any of our results.

In the default scenario, we set $N = 1$, thus assuming that the multiplicity created in each N-N collision is a constant. In real N-N collisions, the multiplicity fluctuates and the relative distribution of multiplicity around the mean value exhibits a near universal behaviour, the so-called KNO scaling [30]. In order to account for this, we also take into account a scenario where N is distributed according to the KNO distribution.

The value of σ is characteristic for the interaction process, and reflects the precise physics of matter production in secondary interactions. General considerations suggest that it should be of the order of the nucleon radius. We test in the following scenarios involving both constant values $\sigma = 0.6$ fm, $\sigma = 1.0$ fm and a Gaussian distribution of width $\Delta\sigma = 0.3$ fm centered around $\sigma = 0.6$ fm.

The events are divided into centrality classes according to the total entropy, which is the closest to the centrality selection in the real experiments. We further checked the sensitivity of the results to the centrality selection, by considering also the selection according to impact parameter, number of collision participants or the number of binary collisions. It turns out that none of these schemes to determine centrality changes our results substantially, i.e. the details of centrality determination do not matter for the question of v_n fluctuations as long as we do not consider ultra-central events.

Given $\rho(x, y)$, we compute the center of gravity of the distribution and shift coordinates such that $(0, 0)$ coincides with the center of gravity. Next we determine the angular orientation of the ε_n plane from

$$\Psi_n = \frac{1}{n} \arctan \frac{\int dx dy (x^2 + y^2) \sin(n\phi) \rho(x, y)}{\int dx dy (x^2 + y^2) \cos(n\phi) \rho(x, y)} + \pi/n \quad (6)$$

and the eccentricity of the event as

$$\varepsilon_n = \frac{\int dx dy (x^2 + y^2) \cos[n(\phi - \Psi_n)] \rho(x, y)}{\int dx dy (x^2 + y^2) \rho(x, y)} \quad (7)$$

Averaging over a large number $O(20.000)$ of events, we determine the mean eccentricity $\langle \varepsilon_n \rangle$ for each centrality class and express the fluctuations in terms of the scaled eccentricity as

$$\delta\varepsilon_n = \frac{\varepsilon_n - \langle \varepsilon_n \rangle}{\langle \varepsilon_n \rangle} \quad (8)$$

where ε_n is the eccentricity determined for a particular event.

III. RESULTS

A. Centrality dependence from the Glauber model

First, we test the centrality dependence of $P(\delta\varepsilon_2)$ of the different initial states given by Eqs. (3)–(5). The distributions are shown in Fig. 1 for several centrality classes and compared to the ATLAS data [27]. The values of the free parameters α , β and f are shown in the figure, and we use $\sigma = 0.4$ fm and $N = 1$. We can make the following observations:

- In the most central collisions all the different models give the same distribution, and is in practice in perfect agreement with the ATLAS data.
- While it was observed in Ref. [25] that the distributions are same for sWN and sBC initializations at RHIC, the same does not hold for the LHC energy due to the larger nucleon-nucleon cross-section. In general sWN initialization at the LHC gives wider distributions than sBC initializations. This difference is even enhanced by the powers in Eqs. (3) and (4) required to reproduce the centrality dependence of the multiplicity.
- Although the binary collision based initialization, Eq. (3), gives a good agreement with the data in the central collisions and the binary/participant mixture, Eq. (5), in the peripheral collisions, none of these simple models can fully account the centrality dependence of the distributions.

B. Initial nuclear geometry

Next, we aim at testing the assumptions for the initial nuclear geometry. In particular we test four different scenarios across the whole centrality range: 1) a standard MC Glauber scenario based on nucleons distributed with a realistic Woods-Saxon nuclear density (Glauber), 2) a standard Glauber scenario based on scattering constituent quarks instead (CQS), 3) a Glauber scenario based on nucleons sampled from a hard sphere distribution (HS) 4) a scenario mimicking strong saturation effects in the initial density based on a 2d nucleon sheet distribution (S). In all these cases, $\sigma = 0.6$ fm and $N = 1$ is assumed. Here, we use simple sBC model, with entropy density directly proportional to the density of the binary collisions.

The centrality dependence of the v_2 or ε_2 fluctuations from the 0-5% most central to 35-40% peripheral collisions is shown for these four different scenarios and compared with ATLAS data in Fig. 2.

Several observations are readily apparent:

- For central collisions, the scaled fluctuations in v_2 become universal, i.e. show the same pattern independent of the underlying geometry. For less central events, differences between the four different scenarios become readily apparent.
- As evidenced by the differences between Glauber and HS, the surface diffuseness of the nucleus is a key parameter determining the width of the distribution.
- As indicated by the differences between HS and sheet, differences in central density are also probed. This suggests a scenario in which the wide fluctuations are driven by nucleons at the edge of one nucleus, passing (for large impact parameters) through the central region of the other nucleus, i.e. what matters is both the probability to have a nucleon far from the center of nucleus A and the effect of its passage through nucleus B. This would suggest that any kind of saturation generically narrows the width of the distribution as compared with an unsaturated scenario.
- The more realistic scenarios Glauber and CQS are closer to the data, but no scenario can account for the full centrality dependence. In particular, Glauber becomes too narrow above 20% centrality and CQS is too wide between 10 and 25% centrality.

We have similarly studied the centrality dependence of v_3 and v_4 fluctuations, however these appear to follow the same generic scaling as observed for v_2 in central collisions and do not allow to distinguish different models.

These results raise the question if a modified version of the Glauber scenario, for instance size scale fluctuations or KNO multiplicity fluctuations could not bring the model in agreement with the data. We explore these possibilities for 5-10% centrality (where the Glauber scenario gives a wider distribution than the data) and for 35-40% centrality (where the width of the data is underestimated).

C. Size scale and multiplicity fluctuations

In Fig. 3, we again consider the sBC Glauber scenario and try variations of the parameter σ which represents the size of the matter spot generated in an individual N-N collision in combination with possible KNO-type multiplicity fluctuations. As the figure demonstrates, there is no significant dependence on either of these factors, in particular no combination of parameters is able to shrink the distribution at central collisions while at the same time widen it at large centralities.

Similar results (not shown here) can be obtained for the CQS scenario.

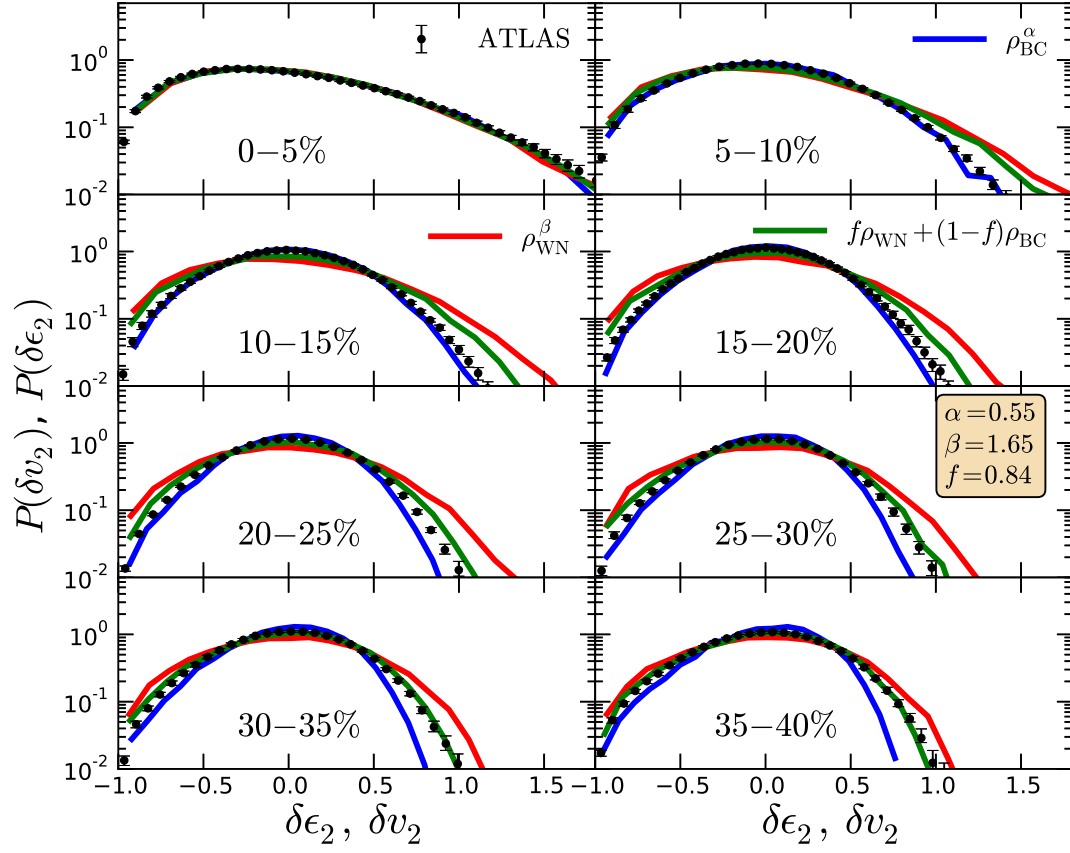


FIG. 1. Centrality dependence of δv_2 or $\delta \epsilon_2$ fluctuations in various scenarios to generate the initial state from the initial nucleon distributions.

D. Surface thickness

In contrast, we demonstrate in Fig. 4 that there is a characteristic dependence of the width of the $P(\delta v_2)$ on the surface diffuseness assumed for the nuclear density distribution Eq. (1) — the distribution widens with increased surface diffuseness and shrinks with decreased surface diffuseness. Of all influences tested for a Glauber model based on colliding nucleons, this is the only one clearly leading to an effect above the statistical uncertainty.

However, even assuming yet unknown physics allows to make the surface diffuseness a free parameter, there are two further obstacles:

- The surface diffuseness always correlates positively with the width of $P(v_2)$. However, the centrality dependence of the mismatch between data and model is non-trivial, i.e. in order to account for the data one would have to assume that the surface diffuseness of a nucleus (which is a property of the particular nucleus) depends on at what impact parameter that nucleus will later collide, which is conceptually very problematic.

- While $P(\delta v_2)$ is constrained to fulfill $\int d\delta v_2 P(\delta v_2) = 1$ and $\int d\delta v_2 \delta v_2 P(\delta v_2) = 0$ by construction, the shape is, given these constraints, free. Looking closely at Fig. 4, one may note that a different value of the surface diffuseness reproduces the left and side and the right hand side of the distribution, i.e. data and model do not match in shape.

IV. CONCLUSIONS

We calculated the centrality dependence of the eccentricity fluctuation spectra from several MC Glauber model based initial states. First, we found that the v_2 fluctuations are universal in the most central collisions, i.e. independent of the model details, and well described by all the models. The same holds for the higher harmonics in all the centrality classes. However, none of the models tested here were able to reproduce the centrality dependence of $P(\delta v_2)$ observed by the ATLAS Collaboration. In particular, a simple mixture of binary collisions and wounded nucleons fails to reproduce the fluctuation spectra, except in the most peripheral centrality classes

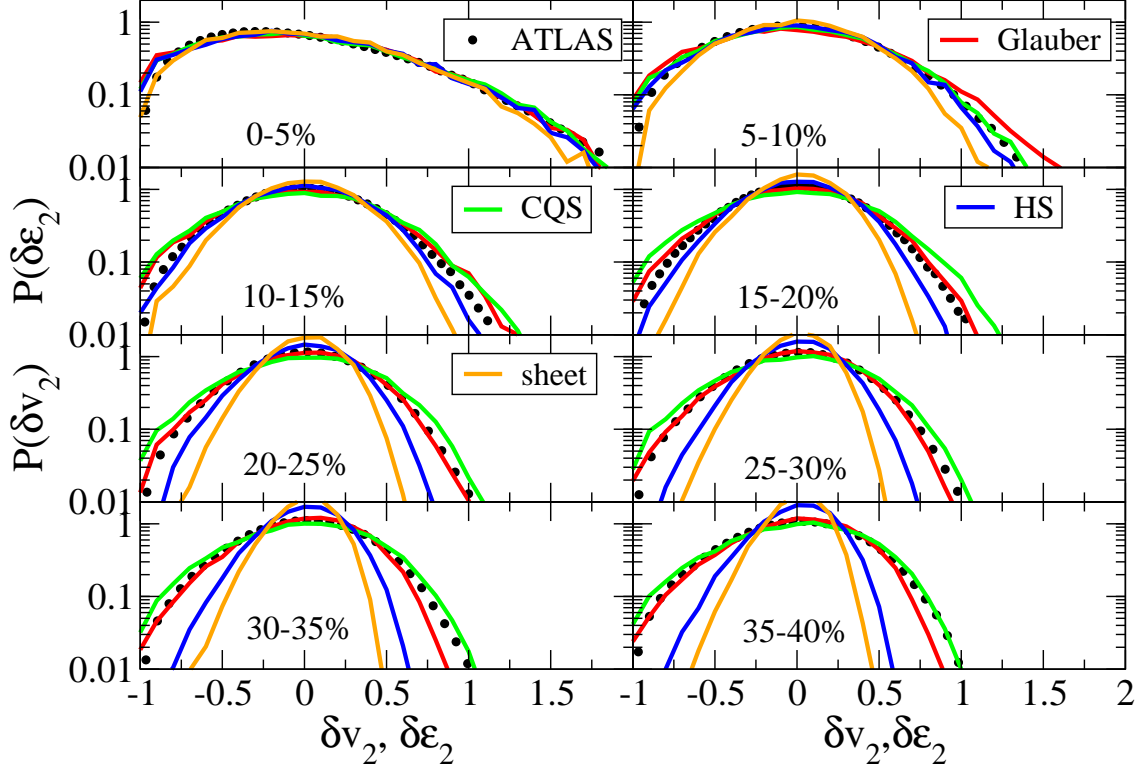


FIG. 2. Centrality dependence of δv_2 or $\delta \epsilon_2$ fluctuations in various scenarios to generate the initial distributions inside the nuclei (see text).

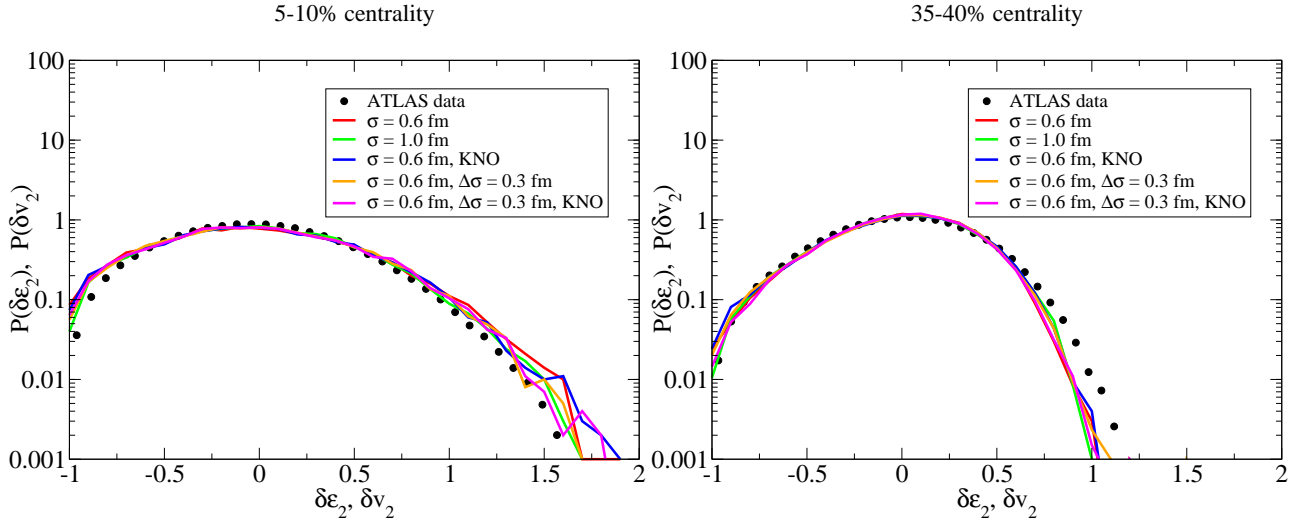


FIG. 3. Dependence of δv_2 fluctuations on multiplicity or N-N collision geometry size scale fluctuations.

considered here.

We also identified several parameters that do not affect the distribution, like KNO fluctuations and the size of the matter spots generated in the individual NN collisions. We further demonstrated that the distributions are sensitive to simple non-linear parametrizations given by Eqs. (3) and (4), as well as by the changes in the initial distributions of the interacting objects.

These findings suggest that the geometrical fluctuations in the positions of the nucleons are not enough to explain the data, but some non-linear dynamics in the creation of the matter and/or additional sources of fluctuations are necessary. Both of these properties are realized in the QCD based initial state models. For example, pQCD + saturation model in Ref. [31, 32] leads to a similar non-linear behavior of the entropy density as Eq. (3)

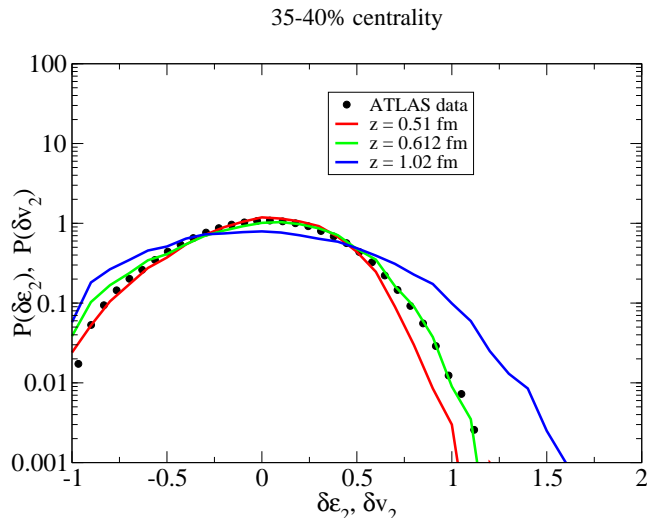


FIG. 4. Dependence of δv_2 fluctuations on the assumed surface diffuseness parameter in the Woods-Saxon model of the nuclear density distribution.

and the sub-nucleon color fluctuations in Refs. [33] presumably lead to a similar effect on the distributions as the CQS model above.

Overall, reproducing the observed centrality dependence of the v_2 fluctuation distributions is a non-trivial task and gives very tight constraints for the modeling of the initial state. All the simple models considered in this work can already be ruled out as valid representations of the initial state geometry.

ACKNOWLEDGMENTS

We thank G. Denicol for useful discussions. This work is supported by the Academy researcher program of the Academy of Finland, Project No. 130472 and the Academy of Finland, Project No. 133005.

-
- [1] M. Strickland, arXiv:1312.2285 [hep-ph].
 - [2] For a recent review and references, see U. W. Heinz and R. Snellings, Annu. Rev. Nucl. Part. Sci. **63**, 123 (2013).
 - [3] P. F. Kolb and U. W. Heinz, In *Hwa, R.C. (ed.) et al.: Quark gluon plasma 3* 634-714.
 - [4] J. -Y. Ollitrault, Phys. Rev. D **46**, 229 (1992).
 - [5] P. Romatschke and U. Romatschke, Phys. Rev. Lett. **99**, 172301 (2007).
 - [6] M. Luzum and P. Romatschke, Phys. Rev. C **78**, 034915 (2008) [Erratum-ibid. C **79**, 039903 (2009)].
 - [7] B. Schenke, S. Jeon and C. Gale, Phys. Rev. Lett. **106**, 042301 (2011); Phys. Rev. C **85**, 024901 (2012); Phys. Lett. B **702**, 59 (2011).
 - [8] C. Gale, S. Jeon, B. Schenke, P. Tribedy and R. Venugopalan, Phys. Rev. Lett. **110**, 012302 (2013).
 - [9] H. Song, S. A. Bass, U. Heinz, T. Hirano and C. Shen, Phys. Rev. Lett. **106**, 192301 (2011) [Erratum-ibid. **109**, 139904 (2012)]; Phys. Rev. C **83**, 054910 (2011) [Erratum-ibid. C **86**, 059903 (2012)].
 - [10] H. Song, S. A. Bass and U. Heinz, Phys. Rev. C **83**, 054912 (2011) [Erratum-ibid. C **87**, 019902 (2013)].
 - [11] C. Shen, U. Heinz, P. Huovinen and H. Song, Phys. Rev. C **82**, 054904 (2010); Phys. Rev. C **84**, 044903 (2011).
 - [12] P. Bozek, Phys. Rev. C **81**, 034909 (2010); Phys. Rev. C **85**, 034901 (2012).
 - [13] P. Bozek and I. Wyskiel-Piekarska, Phys. Rev. C **85**, 064915 (2012).
 - [14] H. Niemi, G. S. Denicol, P. Huovinen, E. Molnar and D. H. Rischke, Phys. Rev. C **86**, 014909 (2012).
 - [15] H. Niemi, G. S. Denicol, P. Huovinen, E. Molnar and D. H. Rischke, Phys. Rev. Lett. **106**, 212302 (2011).
 - [16] U. W. Heinz, J. S. Moreland and H. Song, Phys. Rev. C **80**, 061901 (2009).
 - [17] E. Retinskaya, M. Luzum and J. -Y. Ollitrault, arXiv:1311.5339 [nucl-th].
 - [18] T. Renk, H. Holopainen, U. Heinz and C. Shen, Phys. Rev. C **83** (2011) 014910.
 - [19] T. Renk, H. Holopainen, J. Auvinen and K. J. Eskola, Phys. Rev. C **85** (2012) 044915.
 - [20] C. E. Aguiar, Y. Hama, T. Kodama and T. Osada, Nucl. Phys. A **698**, 639 (2002); O. Socolowski, Jr., F. Grassi, Y. Hama and T. Kodama, Phys. Rev. Lett. **93**, 182301 (2004); R. Andrade, F. Grassi, Y. Hama, T. Kodama and O. Socolowski, Jr., Phys. Rev. Lett. **97**, 202302 (2006); J. Takahashi, B. M. Tavares, W. L. Qian, R. Andrade, F. Grassi, Y. Hama, T. Kodama and N. Xu, Phys. Rev. Lett. **103**, 242301 (2009).
 - [21] B. Alver and G. Roland, Phys. Rev. C **81**, 054905 (2010) [Erratum-ibid. C **82**, 039903 (2010)].
 - [22] G. -Y. Qin, H. Petersen, S. A. Bass and B. Muller, Phys. Rev. C **82**, 064903 (2010) [arXiv:1009.1847 [nucl-th]].
 - [23] Z. Qiu and U. W. Heinz, Phys. Rev. C **84**, 024911 (2011).
 - [24] F. G. Gardim, F. Grassi, M. Luzum and J. -Y. Ollitrault, Phys. Rev. C **85**, 024908 (2012).
 - [25] H. Niemi, G. S. Denicol, H. Holopainen and P. Huovinen, Phys. Rev. C **87**, 054901 (2013).
 - [26] D. Teaney and L. Yan, Phys. Rev. C **86**, 044908 (2012).
 - [27] J. Jia [ATLAS Collaboration], Nucl. Phys. A904-905 **2013**, 421c (2013).
 - [28] A. R. Timmins [ALICE Collaboration], J. Phys. Conf. Ser. **446**, 012031 (2013).
 - [29] H. De Vries, C. W. De Jager and C. De Vries, Atom. Data Nucl. Data Tabl. **36** (1987) 495.
 - [30] Z. Koba, H. B. Nielsen and P. Olesen, Nucl. Phys. B **40** (1972) 317.
 - [31] K. J. Eskola, K. Kajantie and K. Tuominen, Phys. Lett. B **497**, 39 (2001).
 - [32] R. Paatelainen, K. J. Eskola, H. Niemi and K. Tuominen, arXiv:1310.3105 [hep-ph].
 - [33] A. Dumitru and Y. Nara, Phys. Rev. C **85**, 034907 (2012); B. Schenke, P. Tribedy and R. Venugopalan, Phys. Rev. Lett. **108**, 252301 (2012).